Electronic Supplementary Material (ESI) for RSC Advances.

One pot synthesis of NiMo-Al_2O_3 catalysts by solvent-free solid-state method f or hydrodesulfurization

Xiaodong Yi*, Dongyun Guo, Pengyun Li, Xinyi Lian, Yingrui Xu, Yunyun Dong, Weikung Lai, Weiping Fang

National Engineering Laboratory for Green Chemical Productions of Alcohols-Ethers- Esters, College of Chemistry and Chemical Engineering, Xiamen University, Xiamen 361005, China

Table S1 BET properties of Al_2O_3-*x* from analysis of N_2 adsorption-desorption isotherms.

Samples	Al_2O_3–0	Al_2O_3–10	Al_2O_3–15	Al_2O_3–20
S_{BET} ($m^2 \cdot g^{-1}$)	100	257	322	199
V_p($cm^3 \cdot g^{-1}$)	0.25	0.97	0.89	0.56
D_m(nm)	6.3	10.0	8.3	7.9

Table S2 Cl/Al atomic ratio of the oxide and sulfide NiMoAl-*x* catalysts obtain by XPS

Catalysts	Cl/Al ($\times 10^2$) Oxide catalysts	Cl/Al ($\times 10^2$) Sulfide catalysts
NiMoAl-0	5.1	0
NiMoAl-2	2.9	0
NiMoAl-6	2.7	0
NiMoAl-10	2.1	0
NiMoAl-15	1.6	0
NiMo/Al_2O_3	0.2	0

The reaction products of DBT HDS were collected and analyzed by gas chromatography per hour when the steady state had been reached. The various reactant and product species were further verified by an Agilent 6890 GC installed with an MS 80 mass spectrometer. The GC spectra and product distribution of DBT HDS over NiMoAl-15 catalyst were shown in S-Fig. 1. The main product is biphenyl (BP) through the direct desulfurization pathway (DDS), others are cyclohexylbenzene (CHB) and dicyclohexyl (DCH) through the hydrogenation route (HYD).

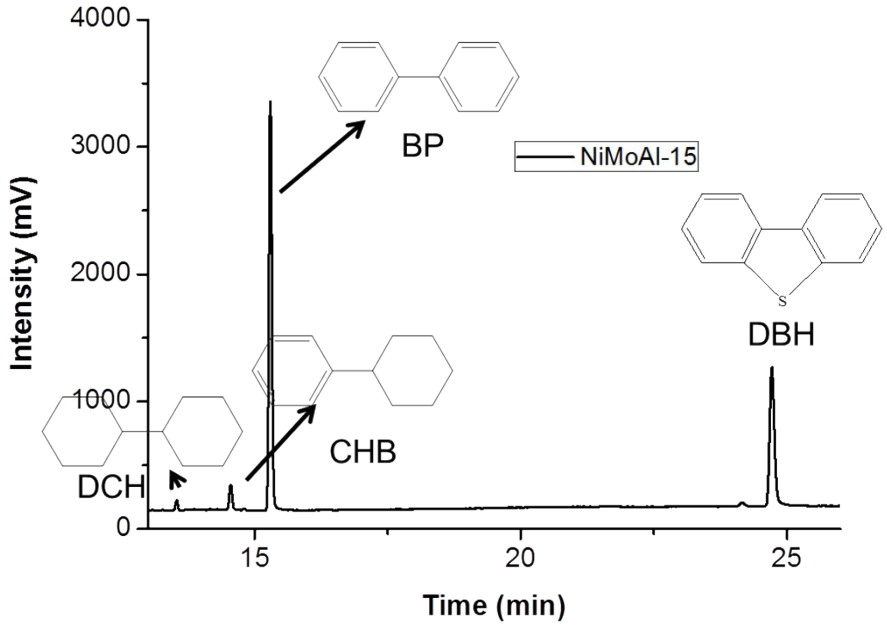

S-Fig. 1 GC spectra of the product distribution of DBT HDS over NiMoAl-15 catalyst.

A series of Al_2O_3-*x* (where *x* represents the weight ratio of PEG to alumina, and *x*=0, 10, 15, 20) were synthesized via solvent-free solid-state route with different PEG addition.

Nitrogen adsorption–desorption isotherms of the Al_2O_3-*x* catalysts are shown in S-Fig. 2. All the samples show type IV isotherms with H1 hysteresis loops, which indicate the feature of mesoporous structure. Texture parameters calculated by BET and BJH methods (Table S2) show that the BET surface area and pore volume increase obviously with increasing PEG addition, which indicates that PEG addition could develop porous system own to its combustion swelling properties. However, when the PEG addition is sufficiently high, swelling is not completely free, but is constrained by steric effects. As a result the BET surface area and pore volume of Al_2O_3-20 decrease compared with the Al_2O_3-15 sample. These results indicate that PEG plays a key role in directing framework of the as-prepared samples.

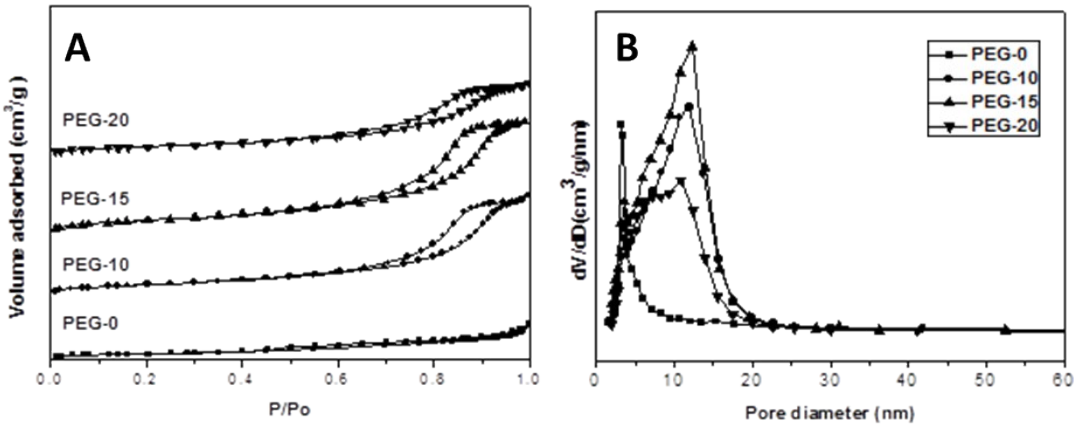

S-Fig.2 (A) N_2 adsorption-desorption isotherms and (B) BJH pore size distribution profiles obtained from Al_2O_3-*x*.

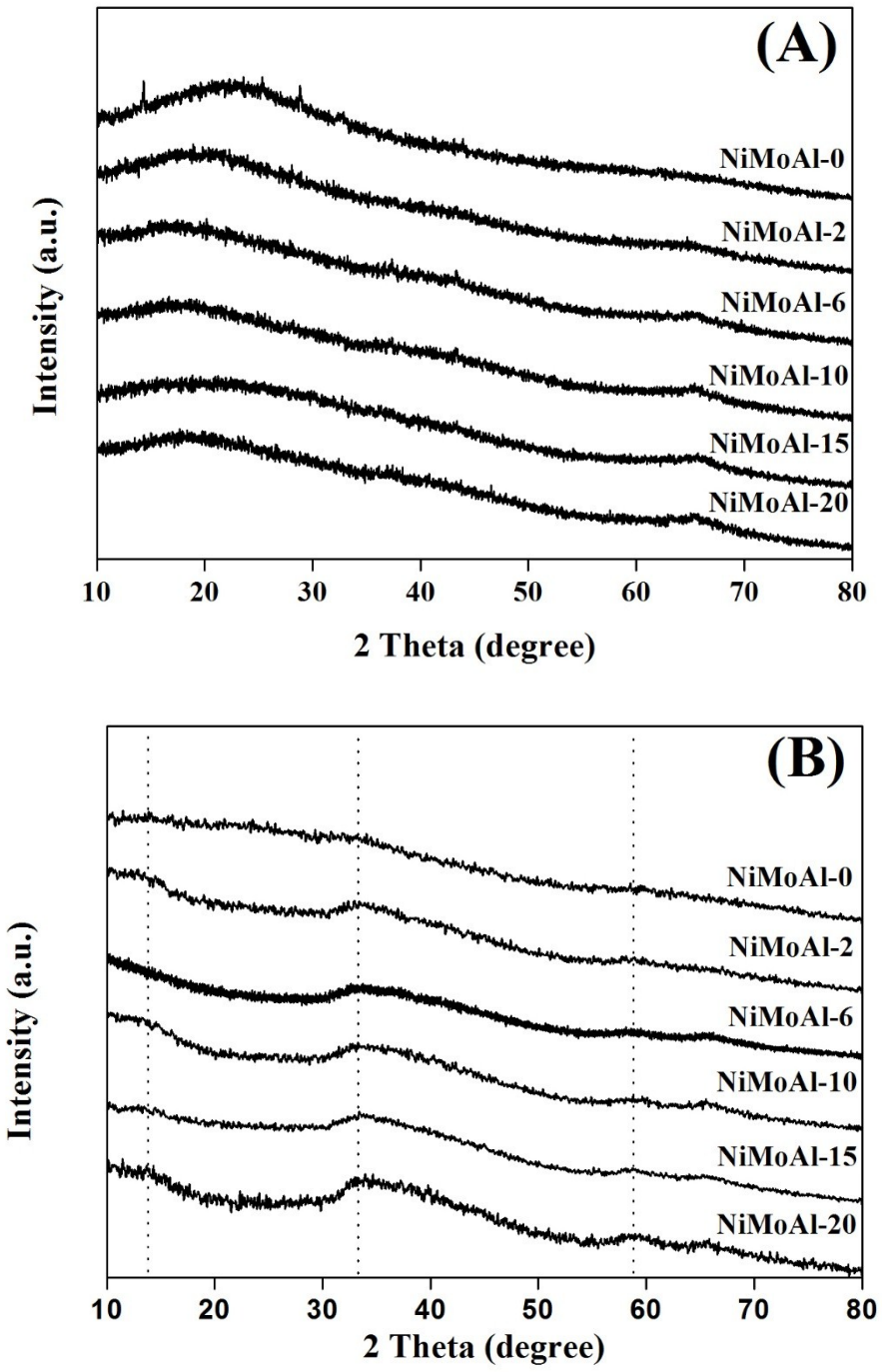

S-Fig. 3 X-ray diffraction patterns of the oxide (A) and sulfide (B) NiMoAl-*x* catalysts.

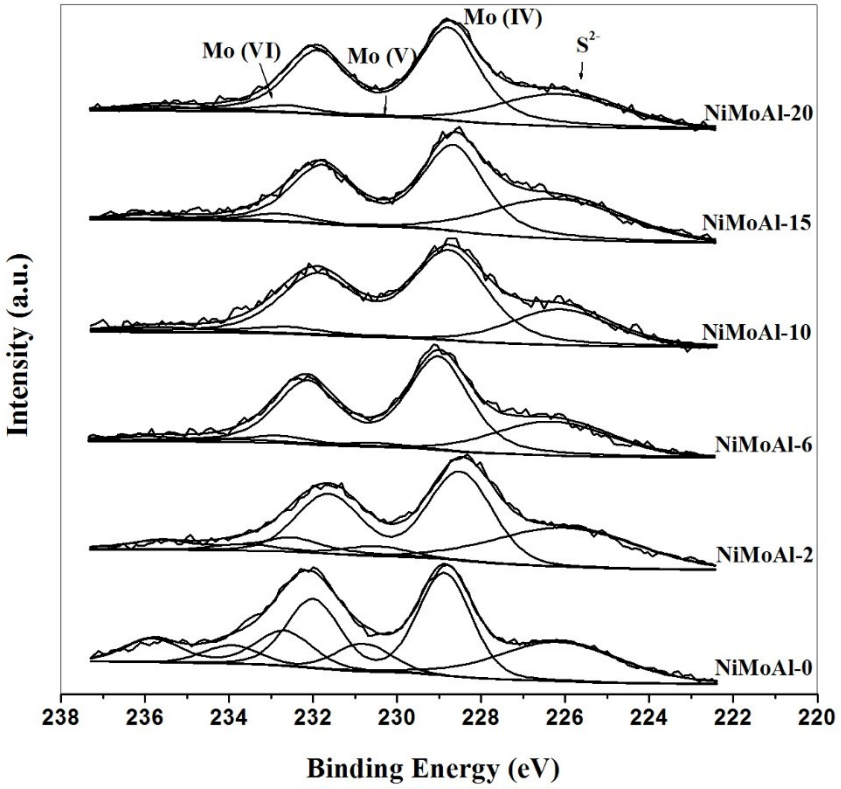

S-Fig. 4 Mo 3*d* spectra of the sulfided NiMoAl-*x* catalysts and their decomposition.

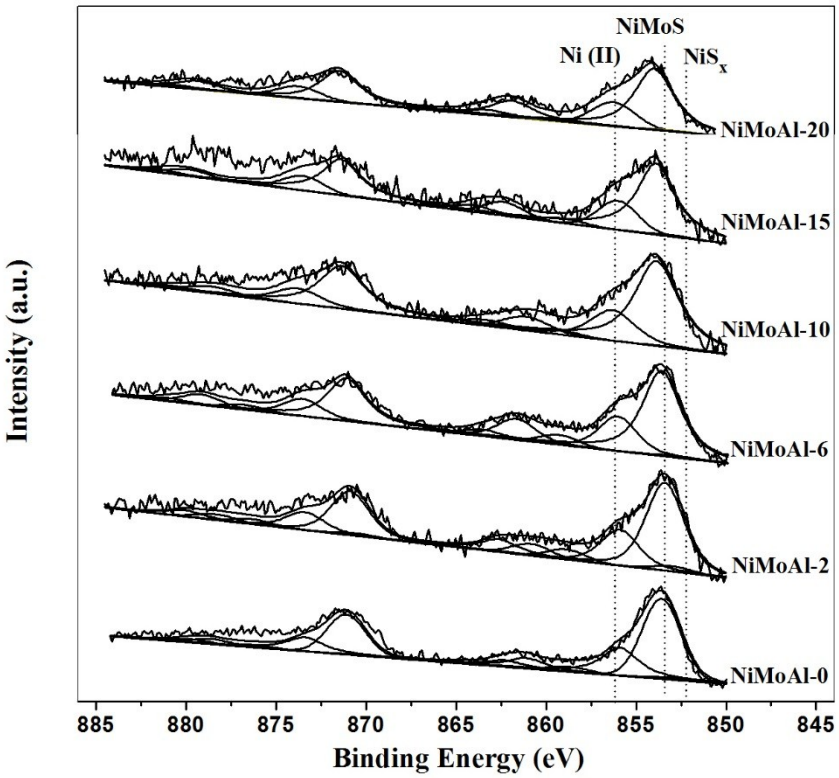

S-Fig. 5 Ni 2*p* spectra of the sulfided NiMoAl-*x* catalysts and their decomposition.

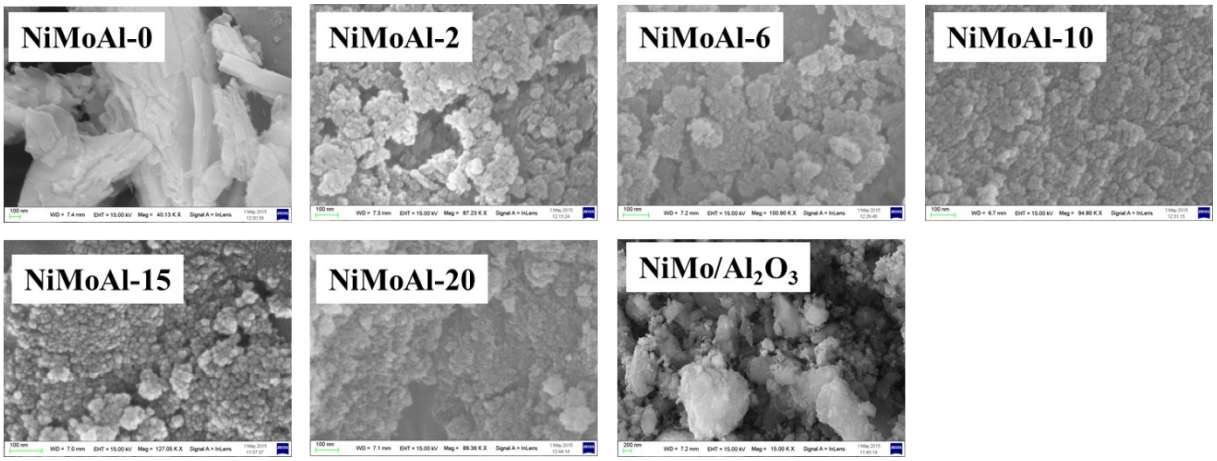

S-Fig.6 SEM images of NiMoAl-*x*(*x*=2, 6, 10, 15, 20) and $NiMo/Al_2O_3$ catalysts.

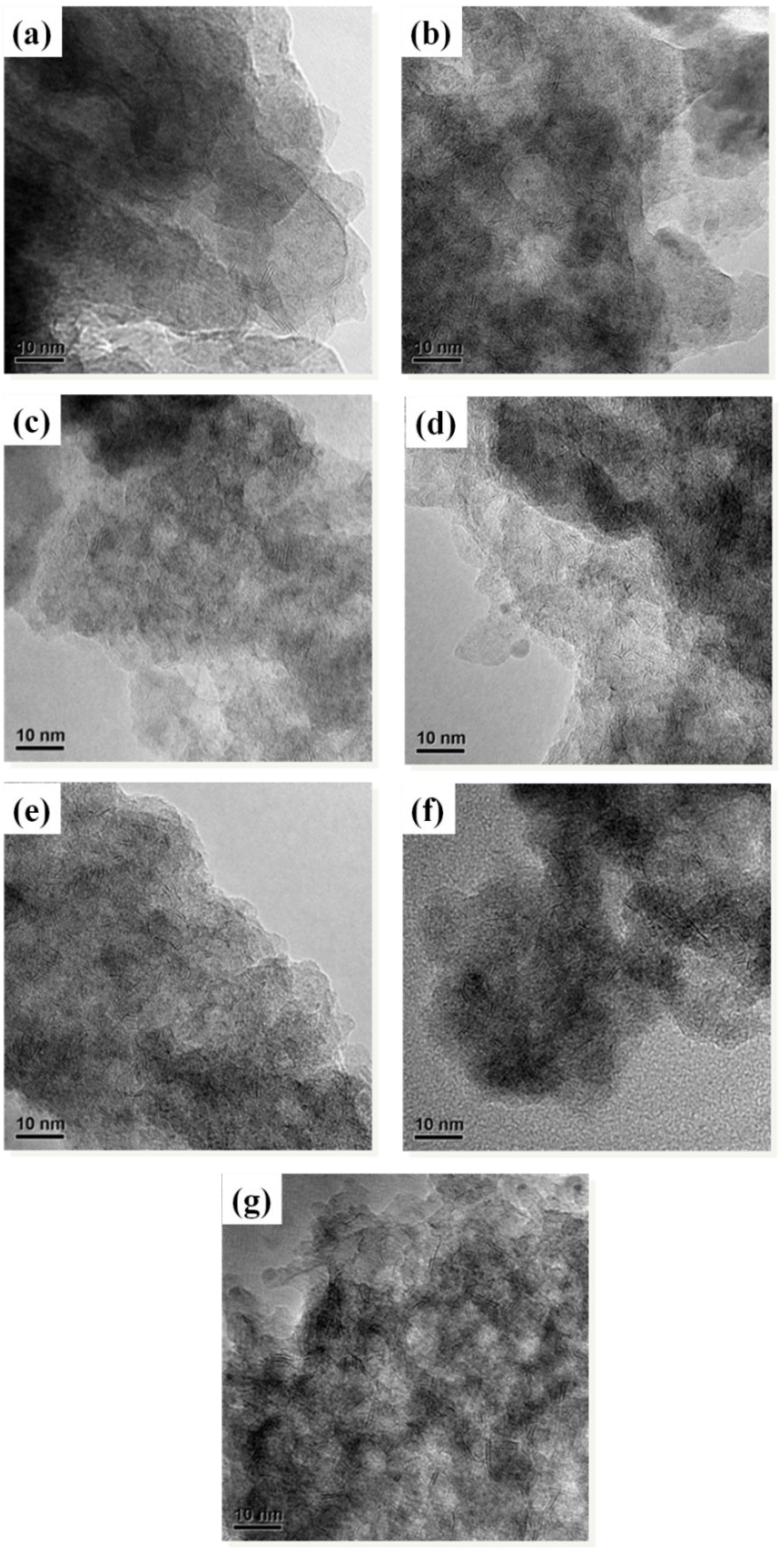

S-Fig. 7 HRTEM images of the sulfided NiMoAl-*x* and NiMo/Al_2O_3 catalysts: (a) NiMoAl-0, (b) NiMoAl-2, (c) NiMoAl-6, (d) NiMoAl-10, (e) NiMoAl-15, (f) NiMoAl-20, and (g) NiMo/Al_2O_3.